Eur. J. Mineral.
2009, **21**, 203–217
Published online November 2008

Characterisation of ballen quartz and cristobalite in impact breccias: new observations and constraints on ballen formation

LUDOVIC FERRIÈRE[1,*], CHRISTIAN KOEBERL[1] and WOLF UWE REIMOLD[2]

[1] Department of Lithospheric Research, University of Vienna, Althanstrasse 14, A-1090 Vienna, Austria
*Corresponding author, e-mail: ludovic.ferriere@univie.ac.at
[2] Museum of Natural History (Mineralogy), Humboldt-University, Invalidenstrasse 43, D-10115, Berlin, Germany

Abstract: Ballen quartz and cristobalite in impactite samples from five impact structures (Bosumtwi, Chicxulub, Mien, Ries, and Rochechouart) were investigated by optical microscopy, scanning electron microscopy (SEM), cathodoluminescence (CL), transmission electron microscopy (TEM), and Raman spectroscopy to better understand ballen formation. The occurrence of so-called ''ballen quartz'' has been reported from about one in five of the known terrestrial impact structures, mostly from clasts in impact melt rock and, more rarely, in suevite. ''Ballen silica'', with either α-quartz or α-cristobalite structure, occurs as independent clasts or within diaplectic quartz glass or lechatelierite inclusions. Ballen are more or less spheroidal, in some cases elongate (ovoid) bodies that range in size from 8 to 214 μm, and either intersect or penetrate each other or abut each other. Based mostly on optical microscopic observations and Raman spectroscopy, we distinguish five types of ballen silica: α-cristobalite ballen with homogeneous extinction (type I); ballen α-quartz with homogeneous extinction (type II), with heterogeneous extinction (type III), and with intraballen recrystallisation (type IV); chert-like recristallized ballen α-quartz (type V). For the first time, coesite has been identified within ballen silica – in the form of tiny inclusions and exclusively within ballen of type I.

The formation of ballen involves an impact-triggered solid-solid transition from α-quartz to diaplectic quartz glass, followed by the formation at high temperature of ballen of β-cristobalite and/or β-quartz, and finally back-transformation to α-cristobalite and/or α-quartz; or a solid-liquid transition from quartz to lechatelierite followed by nucleation and crystal growth at high temperature. The different types of ballen silica are interpreted as the result of back-transformation of β-cristobalite and/or β-quartz to α-cristobalite and/or to α-quartz with time. In nature, ballen silica has not been found anywhere else but associated with impact structures and, thus, these features could be added to the list of impact-diagnostic criteria.

Key-words: ballen quartz, α-cristobalite, silica, shock metamorphism, impact structure.

1. Introduction

1.1. Historical background and previous studies of ballen quartz

So-called ''ballen quartz'' was first observed in 1890, in impact melt rock from the Mien impact structure (Holst, 1890). At this time, the impact origin of Mien was not yet confirmed and consequently these rocks were associated with some kind of volcanic activity. Ballen quartz was described to occur in the form of ''rounded, egg shaped or elongated batches, consisting of aggregates of elongated lamellae'' (Holst, 1890).

Similar features were described much later by McIntyre (1968) from impactites of the Clearwater impact structures and by Engelhardt (1972) from the Ries. The first detailed study of these features was reported by Carstens (1975), who concluded that the ballen texture represented pseudomorphs after cristobalite that had replaced lechatelierite initially formed by shock-induced thermal transformation of quartz. Carstens (1975) also suggested that ballen ''formed as the result of the tensile stresses set up by the high-low inversion of cristobalite being associated with a volume shrinkage of about 7 %''. Bischoff & Stöffler (1984) found that ballen represented recristallized diaplectic quartz glass that had undergone the transition to cristobalite and then to α-quartz. They recognized three types of ''ballen quartz'': (a) ballen with optically homogeneous extinction (~30–45 GPa), (b) ballen with different crystallographic orientations (~45–55 GPa), and (c) ballen with intraballen-recrystallisation (>50 GPa). This is based on optical characteristics of coexisting shock-deformed quartz and feldspar grains, and assigned specific shock pressures to the shock metamorphic stages experienced by the quartz grains now converted to ballen silica.

''Ballen quartz'' has since been observed in samples from many other impact structures (see Table 1), but not many detailed descriptions and characterisations have been published, except for ballen from Popigai (Whitehead *et al.*, 2002) and from Wanapitei (Dressler *et al.*, 1997),

0935-1221/09/0021-1898 $ 6.75
DOI: 10.1127/0935-1221/2009/0021-1898

Table 1. Impact structures in which ballen have been observed so far. Structures with asterisk (*) are those for which thin section samples were investigated here.

Structure name	Location	Diameter (km)	Age (Ma)	Host rock/Types of ballen	Reference
Boltysh	Ukraine	24	65.17 ± 0.64	Microcrystalline melt rock	Grieve *et al.*, 1987
Bosumtwi*	Ghana	10.5	1.07	Suevite (type I)	*e.g.*, Boamah & Koeberl, 2006; Ferrière *et al.*, 2006; this study
Chesapeake Bay	Virginia, U.S.A.	85	35.5 ± 0.3	Suevite (types III and IV)	Bartosova *et al.*, 2007
Chicxulub*	Yucatan, Mexico	180	64.98 ± 0.05	Suevite and impact melt rock (type IV)	*e.g.*, Stöffler *et al.*, 2004; Tuchscherer *et al.*, 2004; Wittmann *et al.*, 2004; this study
Clearwater East	Quebec, Canada	26	290 ± 20	Impact melt rock	McIntyre, 1968
Clearwater West	Quebec, Canada	36	290 ± 20	Impact melt rock	McIntyre, 1968; Phinney *et al.*, 1978
Deep Bay	Saskatchewan, Canada	13	99 ± 4	Intensively shocked granite	Short, 1970
Dellen	Sweden	19	89.0 ± 2.7	Impact melt rock	Carstens, 1975
Dhala	India	15	>1600; <2500	Impact melt rock	Pati *et al.*, in press
El'gygytgyn	Russia	18	3.5 ± 0.5	Impact melt rock (type I)	*e.g.*, Gurov *et al.*, 2005
Gow	Saskatchewan, Canada	4	<250	Impact melt rock	Thomas *et al.*, 1977
Ilynets	Ukraine	8.5	378 ± 5	Shock-melted granitoid clasts (in breccia)	Gurov *et al.*, 1998
Jänisjärvi	Russia	14	700 ± 5	Cryptocrystalline melt breccia	*e.g.*, Müller *et al.*, 1990
Kara	Russia	65	70.3 ± 2.2	Impact melt rock	Schmieder & Buchner, 2007
Lappajärvi	Finland	23	73.3 ± 5.3	Clast-poor impact melt rock (types II, III, and IV)	Carstens, 1975; Bischoff & Stöffler, 1984
Manicouagan	Quebec, Canada	100	214 ± 1	Impact melt breccia	Schmieder & Buchner, 2007
Mien*	Sweden	9	121.0 ± 2.3	Impact melt rock (types I, II, III, and IV)	Holst, 1890; Carstens, 1975; this study
Mistastin	Labrador, Canada	28	36.4 ± 4	Impact melt rock	Grieve, 1975
Morokweng	South Africa	70	145.0 ± 0.8	Partially annealed granite	Reimold *et al.*, 1999
New Quebec	Quebec, Canada	3.44	1.4 ± 0.1	Impact melt rock	Marvin & Kring, 1992
Popigai	Russia	100	35.7 ± 0.2	Impact melt rock (types I, II, III, and IV)	*e.g.*, Vishnevsky & Montanari, 1999; Whitehead *et al.*, 2002
Ries*	Germany	24	15.1 ± 0.1	Impact melt rock from Polsingen and Amerbach (types IV and V)	*e.g.*, Engelhardt, 1972; Osinski, 2004; this study
Rochechouart*	France	25	214 ± 8	Impact melt rock (types III, IV, and V)	Ferrière & Koeberl, 2007; this study
Sääksjärvi	Finland	6	~560	Cryptocrystalline melt breccia	*e.g.*, Müller *et al.*, 1990
Saint Martin	Manitoba, Canada	40	220 ± 32	Impact melt rock	Phinney *et al.*, 1978
Suvasvesi N	Finland	4	<1000	Impact melt rock	Pesonen *et al.*, 1996
Tenoumer	Mauritania	1.9	0.0214 ± 0.0097	Impact melt rock	French *et al.*, 1970; French, 1998
Ternovka (Terny)	Ukraine	11	280 ± 10	Impact melt rock	Schmieder & Buchner, 2007
Tswaing	South Africa	1.13	0.220 ± 0.052	Suevitic gravel	Montanari & Koeberl, 2000
Wanapitei	Ontario, Canada	7.5	37.2 ± 1.2	Glassy impact melt rock (types III and IV)	Grieve & Ber, 1994; Dressler *et al.*, 1997
Zapadnaya	Ukraine	3.2	165 ± 5	Suevite and impact melt rock	*e.g.*, Gurov *et al.*, 2002

Diameter and age data from Earth Impact Database (2008).

where some information on the different types of ballen are reported. Ballen with a ''toasted appearance'' somewhat similar to what has been described for shocked quartz grains (*e.g.*, Short & Gold, 1996) have been described from Popigai (Whitehead *et al.*, 2002), from Wanapitei (Dressler *et al.*, 1997), and more recently from Dhala (Pati *et al.*,

in press). Alpha-quartz, α-cristobalite, and α-tridymite were identified, using X-ray diffraction techniques, in ballen-quartz-bearing melt rocks from Popigai (Vishnevsky & Montanari, 1999; Whitehead *et al.*, 2002).

Short (1970) was able to reproduce ballen-like features experimentally, after annealing of a slab of experimentally shocked (at ~40 GPa) quartzite at 1450 °C for 24 h, producing ''ovoid to arcuate microstructures'' within grains of diaplectic silica glass. In these experiments, an embryonic stage of ''ballen quartz'' formed already in the specimens annealed at 1200 °C. Short (1970) concluded that ''ballen quartz'' was formed by recrystallisation of glassy material at high temperatures. Similar annealing experiments with diaplectic quartz glass by Rehfeldt-Oskierski (1986) arrived at comparable results, with a minimum annealing temperature of 1150 °C for ballen to develop. Ballen formed at 1150 and 1300 °C were 0.2–0.3 mm and 0.5–1.0 mm in size, respectively. Polycrystalline ballen with individual crystals of 0.1–0.4 mm in size were also produced (Rehfeldt-Oskierski, 1986). In addition, the occurrences of ''patches of faint planar fractures'' (Short, 1970) or ''relics of planar deformation features (PDFs)'' (Rehfeldt-Oskierski, 1986) within the annealed samples are mentioned, as observed by these workers through optical microscopy.

1.2. Occurrence of ballen quartz and cristobalite

Ballen silica has been reported from about one in five of the known terrestrial impact structures (Table 1), mostly from impact melt rock and, more rarely, from suevite samples. These occurrences include the Bosumtwi, Chicxulub, Mien, Ries, and Rochechouart impact structures, from which samples have been investigated here (Fig. 1). We present a detailed study of 27 thin sections of samples from these impact sites, to contribute to the understanding of the so far still uncertain formation mechanism(s) of ''ballen quartz''.

2. Samples and geological background for studied impact structures

Our classification of the various rock types follows definitions by Stöffler & Grieve (2007). Impactite is defined as ''rock produced by impact metamorphism'', including ''shocked rocks, impact breccias, impact melt rocks, (micro)tektites and impactoclastic air fall beds'' (Stöffler & Grieve, 2007). Suevite (or suevite breccia) is defined as a ''polymict impact breccia with particulate matrix containing lithic and mineral clasts in all stages of shock metamorphism including cogenetic impact melt particles which are in a glassy or crystallized state'' (Stöffler & Grieve, 2007).

Distinction between ''diaplectic quartz glass'' and ''lechatelierite'' is based on morphology, as it is generally accepted that diaplectic quartz glass preserves pre-shock morphology of crystals, whereas the morphology of lechatelierite inclusions is determined by the surface tension of the liquid (*e.g.*, Engelhardt & Stöffler, 1968). Where the terms ''cristobalite''

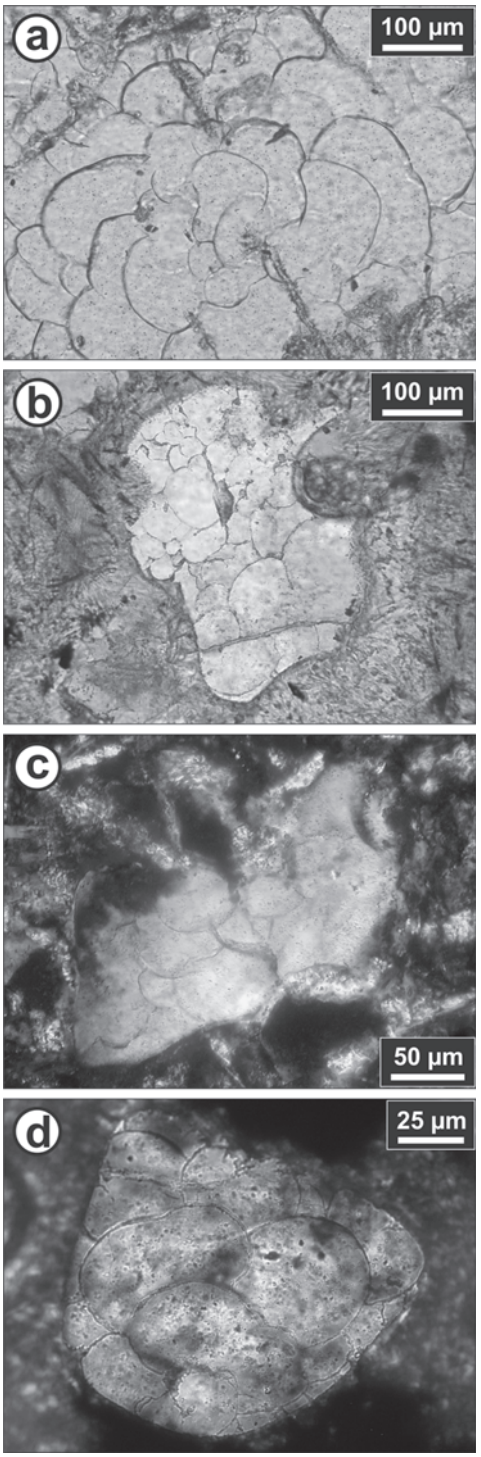

Fig. 1. Microphotographs of ballen silica from various impact structures. (a) Elongate ovoid (crescent) to roundish α-cristobalite ballen in suevite from Bosumtwi (sample BH1-0790). (b) Ballen α-quartz with varied ballen sizes in a lechatelierite clast in impact melt rock from Mien. The melt matrix is mostly composed of feldspar, pyroxene, and opaque microlites, with interstitial mesostasis (sample RD_01). (c) Ballen α-quartz in a lechatelierite clast in impact melt rock from Rochechouart (sample 215_5). (d) Roundish to ovoid ballen α-quartz in suevite from Chicxulub (sample Yax-1_808.87m). Microphotographs (a) and (b) taken in plane-polarized light, (c) and (d) in cross-polarized light.

and ''quartz'' are referred, for example with respect to historical observations, it is understood that the low-temperature polymorphs ''α-cristobalite'' and ''α-quartz'' are meant.

2.1. Bosumtwi impact structure (Ghana)

The 1.07 Ma old Bosumtwi crater in Ghana (West Africa) is a well-preserved complex impact structure, 10.5 km in diameter (*e.g.*, Koeberl & Reimold, 2005). Suevite occurs outside of the northern and southern crater rim and contains abundant impact-melt fragments and a variety of clasts up to about 40 cm in size (Boamah & Koeberl, 2006). Coherent impact melt rock has not been found yet at Bosumtwi. ''Ballen quartz'' was observed in some samples from suevite deposits outside the crater rim (Boamah & Koeberl, 2006; Karikari *et al.*, 2007). Recent work on suevite samples from the deep crater moat and the central uplift of the structure, from the LB-O7A and LB-O8A boreholes of the International Continental Scientific Drilling Program (ICDP), have, to date, not revealed the presence of ballen silica (Coney *et al.*, 2007; Ferrière *et al.*, 2007). For this study, we have investigated seven thin sections of suevite samples (BH1-0790, BH1-0790b, BH1-0800, LB-40B, LB-44B, LB-44B2, and LB-48) from the deposit outside the northern crater rim (located 6°33.9′ N and 1°23.9′ W).

2.2. Chicxulub impact structure (Mexico)

The 65 Ma old Chicxulub impact structure located on the Yucatán Peninsula, Mexico, has a diameter of ~180–195 km (*e.g.*, Hildebrand *et al.*, 1991). Actually covered by post-impact Tertiary sediments, the structure is only accessible by drilling or geophysical techniques. The 1511 m deep ICDP Yaxcopoil-1 (Yax-1) borehole allowed to recover 795 m of post-impact sediments, 100 m of allochthonous polymict impact breccia (mainly suevite), and more than 600 m of displaced target rocks with impact-induced dike breccias (Stöffler *et al.*, 2004). Rare ''ballen quartz'' in silica inclusions was mentioned in some samples of the allochthonous polymict impact breccia (*e.g.*, Stöffler *et al.*, 2004; Tuchscherer *et al.*, 2004; Wittmann *et al.*, 2004). We investigated six thin sections of samples from the Yax-1 drill core (suevite samples from 808.87, 842.51, 852.80, 860.25, and 889.32 m depth; and a brecciated impact melt rock sample from 875.35 m depth).

2.3. Mien impact structure (Sweden)

The Mien impact structure, 121 ± 2.3 Ma old, has a diameter of about 9 km. It is located in the Transscandinavian Granite Porphyry Belt, in southeastern Sweden (Åström, 1998). Boulders of impactite (mostly impact melt rock), first described as rhyolite of volcanic origin (Holst, 1890), occur to the south of Lake Mien as glacial deposits and on the island of Ramsö. Mien impact melt rock is vesicular and consists mainly of feldspar crystals with intersertal texture, quartz grains and aggregates, pyroxene, hematite, rutile, and ilmenite, with interstices filled by a brownish devitrified mesostasis. Quartz inclusions, partially resorbed along the edges, are generally relict phases that display either PDFs or ''ballen quartz''. We studied five thin sections of impact melt rock from the glacial deposits south of Lake Mien (Mien_01; 02; 02b; RD_01; RD_02).

2.4. Ries impact structure (Germany)

The Ries impact structure, 24 km in diameter and 14.3 ± 0.2 Ma old (Buchner *et al.*, 2003), is a well-preserved complex impact structure in Bavaria (*e.g.*, Pohl *et al.*, 1977). ''Ballen quartz'' has been observed only in Ries impact melt rock (Engelhardt, 1972), mainly in samples from Polsingen and Amerbach (*e.g.*, Carstens, 1975; Osinski, 2004). Three thin sections of impact melt rock from Polsingen (R_POL_1; R_POL_2; SIE_9766) were investigated. Polsingen melt rock is reddish in colour, vesicular, and contains abundant shocked clasts of crystalline basement rocks. The groundmass consists mainly of feldspar phenocrysts, quartz, and cryptocrystalline oxides with an interstitial glassy mesostasis.

2.5. Rochechouart impact structure (France)

The 214 ± 8 Ma old (Kelley & Spray, 1997) Rochechouart impact structure occurs in the northwest of the French Massif Central and has a diameter of about 25 km (*e.g.*, Kraut, 1970; Kraut & French, 1971; Lambert, 1977). Four impactite types have been recognized (*e.g.*, Kraut, 1970; Kraut & French, 1971): impact melt rock, two types of suevite, and one type of polymict lithic breccia. ''Ballen quartz'' in impactite from the Rochechouart structure was only found recently in impact melt rock (Ferrière & Koeberl, 2007). It is a vesicular impact melt rock, which consists mainly of feldspar and pyroxene laths in a matrix of devitrified glass. Rare clasts of shocked quartz and feldspar occur, and a few recristallized quartz clasts show ballen texture. Six thin sections of impact melt rock were investigated (215_2; 3; 3b; 4; 5; B – Muséum National d'Histoire Naturelle, Paris, France).

3. Experimental Methods

The 27 thin sections of impact melt rock and suevite were examined with an optical microscope in both transmitted and reflected light. Some sections were then selected for scanning electron microscopy (SEM), cathodoluminescence (CL), and micro-Raman spectroscopy. One sample (LB-44B sample, from Bosumtwi) was investigated using transmission electron microscopy (TEM).

The sections were carbon-coated and examined with an Oxford Mono-CL system attached to a JEOL JSM 6400 scanning electron microscope at the Department of Mineralogy, Natural History Museum, Vienna, Austria. The operating conditions for all SEM-CL investigations were 15 kV accelerating voltage, 1.2 nA beam current, and

monochromator grating with 1200 lines/mm; CL images were obtained from areas of approximately 450 × 450 μm, with scanning times of about 1 min.

Raman spectra were obtained with a Renishaw RM1000 confocal edge filter-based micro-Raman spectrometer with a 20 mW, 632.8 nm He-Ne-laser excitation system, a grating with 1200 lines/mm, and a thermoelectrically cooled CCD array detector at the Institute of Mineralogy and Crystallography, University of Vienna, Vienna, Austria. Spectra were obtained in the range from 30 to 1000 cm^{-1}, with a 300 s acquisition time. The spectral resolution of the system (apparatus function) was 4.5 cm^{-1} and the wavenumber accuracy was better than ± 1 cm^{-1} (both calibrated with the Rayleigh line and the 520.5 cm^{-1} line of a silicon standard). The Raman spectra were taken in confocal mode from 3 × 3 × 3 μm sample volumes, using a Leica DMLM microscope and a Leica 50 × /0.75 objective, from polished thin section surfaces. Instrument control and data acquisition were done with the Grams/32 software (Thermo Galactic Corporation). For phase identification, reference spectra from Caltech, California Institute of Technology, USA were used (http://minerals.gps.caltech.edu/files/raman/Caltech_data/index.htm accessed 12 October 2007).

The Focused Ion Beam (FIB) technique was used for the preparation of a TEM foil at the GeoForschungsZentrum (GFZ) Potsdam (Germany). A FIB foil of 15 × 5 μm extent and about 150 nm thickness was prepared following the method described by Wirth (2004). Transmission electron microscopy was done with a 200 kV PHILIPS CM 20 STEM equipped with a TRACOR Northern energy-dispersive X-ray detector sensitive to elements with atomic numbers >5 at the Museum of Natural History, Humboldt-University, Berlin (Germany). Conventional bright-field imaging techniques were used to observe and characterize microstructural characteristics of individual ballen.

4. Results

Based mostly on optical microscopic observations and Raman investigation, we recognize five different types of ballen: α-cristobalite ballen with homogeneous extinction (type I); ballen α-quartz with homogeneous extinction (type II), with heterogeneous extinction (type III), and with intraballen recrystallisation (type IV); chert-like recristallized ballen α-quartz (type V; Table 2).

4.1. Optical microscopic observations

Results of the microscopic examination of ballen from these different impact structures are reported separately for each location, in order to distinguish the particularities of ballen from each of these impact sites. General views of ballen from some of our samples are illustrated in Fig. 1. Figure 2 shows impressions of α-cristobalite ballen in a large silica clast. Different types of ballen quartz/cristobalite are presented in Fig. 3.

Table 2. Classification of the different types of ballen according to their microscopic properties and respective characteristics.

Type	Proposed name	Characteristics
I	Alpha-cristobalite ballen with homogeneous extinction	All ballen are isotropic in cross-polarized light; coesite occurs in the form of tiny inclusions within ballen
II	Ballen quartz with homogeneous extinction	All individual ballen have common extinction
III	Ballen quartz with heterogeneous extinction	Each individual ballen has homogeneous extinction
IV	Ballen quartz with intraballen recrystallisation	Intraballen polycrystallinity; heterogeneous extinction within single ballen
V	Chert-like recristallized ballen quartz	Ballen are completely recristallized; rims of individual ballen not easily distinguished in cross-polarized light

Note that all types of ballen quartz are made of alpha-quartz.

4.1.1. Bosumtwi samples

Ballen silica occurs in Bosumtwi samples only in impact melt clasts within suevite samples. It occurs in both diaplectic quartz glass (Fig. 2) and lechatelierite inclusions (Fig. 1a and 4). Ballen display a variety of shapes, from circular to oval or crescent shaped (Fig. 1a, 2, and 3a, b). All individual ballen are composed of α-cristobalite (confirmed with Raman spectroscopy), are isotropic in cross-polarized light (Fig. 3b), and have sharp outlines due to the marginal presence of phyllosilicate minerals (Fig. 2f; phyllosilicates cannot be resolved using optical microscopy but have been characterized by TEM analysis, see below). Only ballen silica of type I has been observed in Bosumtwi samples (Table 2). Most of the ballen contain one or several highly refractive, light green, tiny inclusions (Fig. 2e) that were confirmed as coesite by Raman spectroscopy. Ballen diameters range from 8 to 214 μm, with an average diameter of 50 μm ($n = 478$; 18 clasts). The ballen size distribution is also highly variable from inclusion to inclusion, ranging from inclusions with ballen of similar size to inclusions with a large variation of ballen sizes. However, we have observed a decrease of the average diameter of ballen with increasing number of ballen loops in a given inclusion. No correlations seem to exist between the number of ballen per inclusion and the area of the entire inclusion, and between the average radius of ballen and the inclusion area. Large ballen occur in some inclusions preferentially within peripheral areas, but can also be concentrated in the centre of silica inclusions in other cases.

To complete our observations on ballen at the Bosumtwi impact structure, two polished thin sections (LB-44B and LB-44B2; oriented perpendicular to each other) of the same large (22 mm) silica clast were investigated (Fig. 2). In both thin sections, ballen have more or less

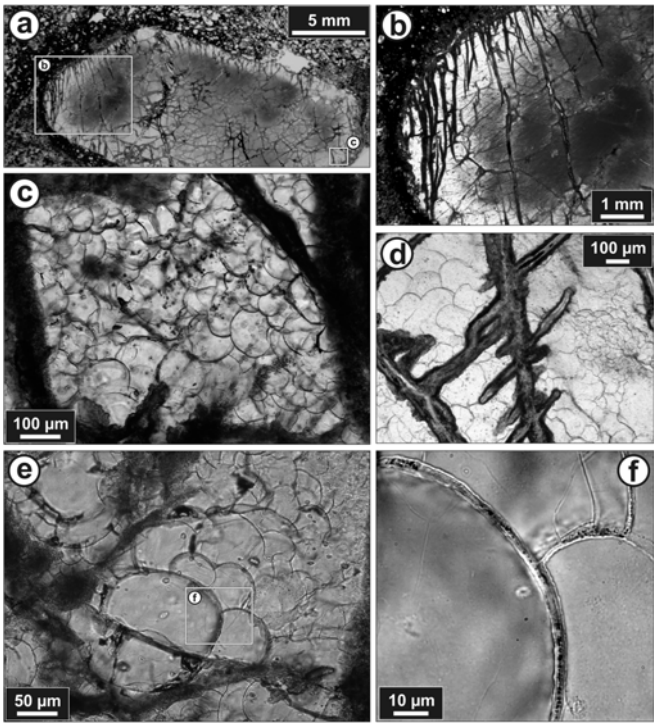

Fig. 2. Microphotographs (in plane-polarized light) of α-cristobalite ballen (type I) in suevite from Bosumtwi (sample LB-44B). (a) General view of a large, shocked silica clast. Primary shape of the quartz grain is preserved. (b) Enlarged part of the silica clast (a) showing the transition from the brownish core (coesite) to the transparent diaplectic quartz glass with fractures and abundant α-cristobalite ballen. (c) Enlarged part of (a) with roundish α-cristobalite ballen (like ''bunches of grapes'') surrounded by fractures/veinlets of in part altered coesite (dark). (d) Fractures/veinlets of altered coesite with secondary α-quartz in the peripheral zone and α-cristobalite ballen in between. (e) A close-up view of well-developed α-cristobalite ballen. Tiny inclusions/grains of coesite (greenish inclusions with high relief) occur within individual ballen. (f) Higher magnification view of the boundary between several ballen, filled here with phyllosilicate.

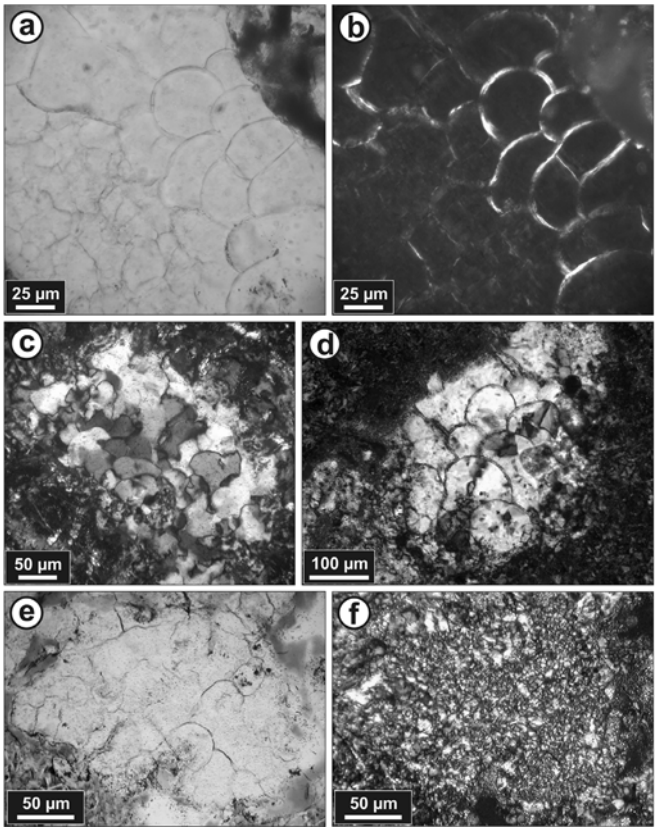

Fig. 3. Microphotographs of various types of ballen quartz/cristobalite. (a) Plane-polarized light and (b) cross-polarized light microphotographs of α-cristobalite ballen (type I) in a lechatelierite clast in suevite from Bosumtwi (sample LB-40B). All individual ballen have common extinction. (c) Ballen α-quartz with heterogeneous extinction (different optical orientations; type III) in a lechatelierite clast in impact melt rock from Rochechouart (sample 215_B; cross-polarized light). Note that each individual ballen has homogeneous extinction. (d) Ballen α-quartz with intraballen recrystallisation (type IV) in a lechatelierite clast in impact melt rock from the Ries (sample SIE-9766; cross-polarized light). Note the intraballen polycrystallinity and the resulting heterogeneous extinction within single ballen. (e) Plane-polarized light and (f) cross-polarized light microphotographs of chert-like recristallized ballen α-quartz (microcrystalline quartz; type V) in a lechatelierite clast in impact melt rock from Rochechouart (sample 215_3). Note that rims of individual ballen are not easily distinguished in cross-polarized light.

roundish shapes, which allows us to visualize ballen as spheroidal bodies. This large silica clast which does not show any indications of deformation or flow in the fluid state (Fig. 2a) is composed of remnants of diaplectic quartz glass, α-cristobalite ballen, and coesite (Fig. 2 and 5a–c). Diaplectic quartz glass is crosscut by several fractures/veinlets that are greenish to brownish in colour (Fig. 2). The fractures contain some phyllosilicate minerals as well as coesite, which is largely recristallized to secondary α-quartz. Coesite occurs also as highly refractive, light green aggregates (up to 30 µm) within the diaplectic quartz glass (Fig. 5a, b; as also described earlier by *e.g.*, Stöffler, 1971; French, 1998; Stähle *et al.*, 2008). Very well developed α-cristobalite ballen occur mainly at the fringe of the silica clast (Fig. 2c), but also along fractures in the inner part of the clast (Fig. 2d). In addition, ballen at the embryonic stage have been observed along fractures and within diaplectic quartz glass (Fig. 5a, b).

4.1.2. Chicxulub samples

Ballen quartz from the Chicxulub impact structure occurs mostly in lechatelierite inclusions (rarely in diaplectic quartz glass) in suevite samples, as well as in the so-called brecciated impact melt rock (unit 5 of Stöffler *et al.*, 2004). Ballen are mainly circular or ovoid in shape (Fig. 1d), with a maximum size measured of 105 µm, and all display heterogeneous extinction of ballen (type IV; Table 2). They exclusively consist of α-quartz. One particularity of the ballen quartz from Chicxulub is that frequently ballen are not obvious when using an optical microscope, possibly because of the absence of phyllosilicate minerals at the margin of the ballen.

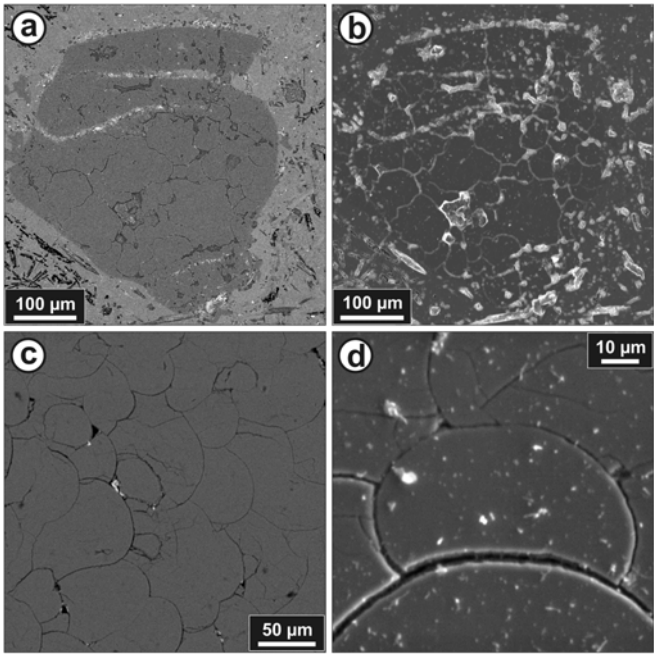

Fig. 4. Backscattered electron (BSE) and secondary electron (SE) images of typical ballen silica. (a) BSE and (b) SE images of an inclusion of lechatelierite displaying ballen α-quartz in a partly crystalline matrix. The sharp boundary between the inclusion and the matrix is obvious. Sample Mien-02. (c) BSE image of ballen at higher magnification showing the very homogeneous composition of individual ballen made of pure SiO_2. Sample LB-44B. (d) SE image showing the ''contact zone'' between individual ballen. Note that the boundary appears empty, whereas in many other cases, phyllosilicate minerals occur. Sample LB-44B.

4.1.3. *Mien samples*

Ballen α-quartz and α-cristobalite occur in Mien impact melt rock samples, mostly in lechatelierite inclusions (Fig. 1b and 4a, b). Most of the ballen are oval to circular in shape and show a large variation in size, from about 22 to 138 µm. Ballen are of types I, II, III, and IV (Table 2); α-cristobalite ballen (type I) occur only associated with ballen α-quartz of type II in the same inclusions. Frequently, a dark ''glass-rich'' halo surrounds the ballen silica inclusions in the melt matrix, but no resorption of the silica inclusion at the contact zone is visible. Ballen silica also occurs within porphyroclasts of granitoid melt, with tail edges made of feldspar glass. Other porphyroclasts contain partially fused quartz grains that display PDFs. Rare quartz glass inclusions with both, ballen silica and crystalline relic areas with PDFs have been observed.

4.1.4. *Ries samples*

In Ries samples, ballen quartz occurs in clasts within impact melt rock and in most cases shows intraballen recrystallisation (type IV; Fig. 3d). Ballen α-quartz of type V (Table 2) has been observed as well. No α-cristobalite ballen has been observed in our Ries samples. Most ballen are circular in shape, but some oval ones occur as well (Fig. 5d). The maximum size measured is 168 µm. No ballen silica has been recognized so far in suevites from either within or outside of the Ries.

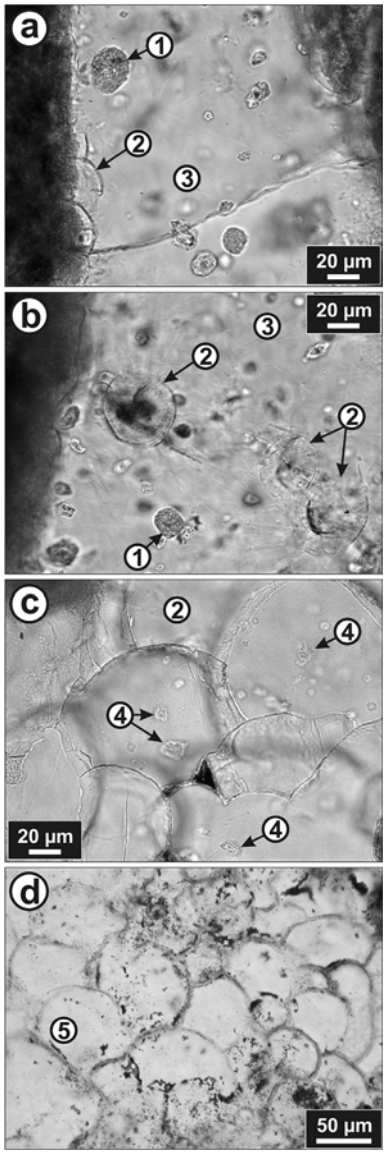

Fig. 5. Microphotographs (in plane-polarized light) of some silica phases investigated with a micro-Raman spectrometer. (a–b) Aggregates/clusters of coesite [1] and incipient development of α-cristobalite ballen [2] in diaplectic quartz glass [3]. (c) Alpha-cristobalite ballen [2] with a few minute inclusions of coesite ± α-quartz [4]. (d) Ballen made of α-quartz [5] in a lechatelierite clast in impact melt rock. All microphotos are from sample LB-44B (from Bosumtwi), with the exception of (d) from sample SIE-9766 (from the Ries). See corresponding spectra in Fig. 7.

4.1.5. *Rochechouart samples*

Three different types of ballen quartz occur in clasts in impact melt rock from the Rochechouart impact structure, namely types III, IV, and V (Table 2). Ballen α-quartz with intraballen recrystallisation (type IV; Fig. 3c) and chert-like recristallized ballen α-quartz (type V; Fig. 3e, f) are the

most common types. No α-cristobalite ballen have been observed in our Rochechouart samples. Most of the ballen are oval shaped (Fig. 1c), and rarely circular. Typically, ballen range in size from about 15 to 90 μm. Regarding the chert-like recristallized ballen α-quartz, rims of individual ballen are not easily distinguished in cross-polarized light.

4.2. Scanning electron microscope and cathodoluminescence observations

The SEM and CL investigations (Fig. 4) show that individual ballen are homogeneous in composition and made of pure SiO_2 (Fig. 4c). The typical pattern of ballen silica is visible in both backscattered electron (BSE) and secondary electron (SE) images (Fig. 4a, b). The BSE image (Fig. 4a) clearly shows the irregular shape of lechatelierite inclusions in a partly crystalline matrix (mainly feldspar crystals in black). The boundaries between ballen appear darker on BSE images, due mostly to the presence of phyllosilicate minerals and/or empty space. The sharp "contact zone" between individual ballen is shown in an SE image at higher magnification (Fig. 4d). Ballen silica does not show distinct CL signatures, reflecting the homogeneity in composition of the ballen, even at the trace-element level.

4.3. Micro-Raman spectroscopy

Silica shows abundant polymorphism as a function of pressure and temperature conditions (Fig. 6). Polymorphs can be easily distinguished using Raman spectroscopy (*e.g.*, Boyer *et al.*, 1985; Stähle *et al.*, 2008; and references therein). During our investigations, α-quartz, diaplectic quartz glass, α-cristobalite, and coesite have been characterized.

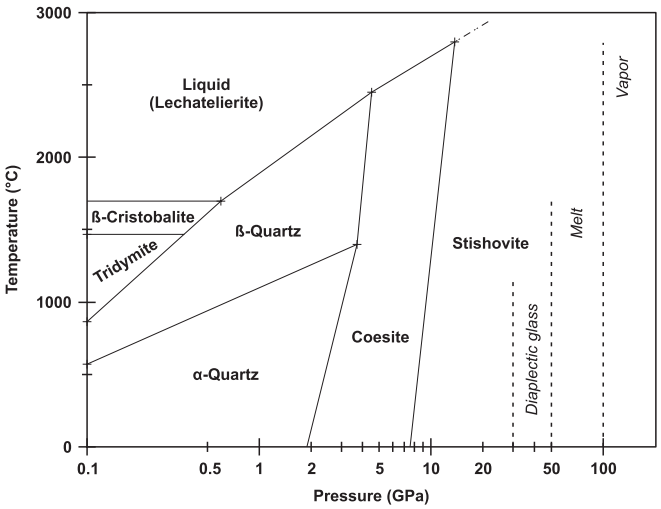

Fig. 6. Combined low and high *P–T* phase diagram of SiO_2 based on static compression experiments for low-pressure transitions (values from Heaney, 1994) and shock experimental data for high-pressure transformations (data from Cohen & Klement, 1967; Jackson, 1976; Kanzaki, 1990). The coesite-stishovite-liquid triple point is after Zhang *et al.* (1993). Approximate threshold pressure for formation of specific shock effects are indicated by vertical dashed lines (after French, 1998).

Corresponding Raman spectra from our natural samples are shown in Fig. 7.

Characteristic Raman spectra of α-cristobalite have been acquired for ballen from the Mien and Bosumtwi

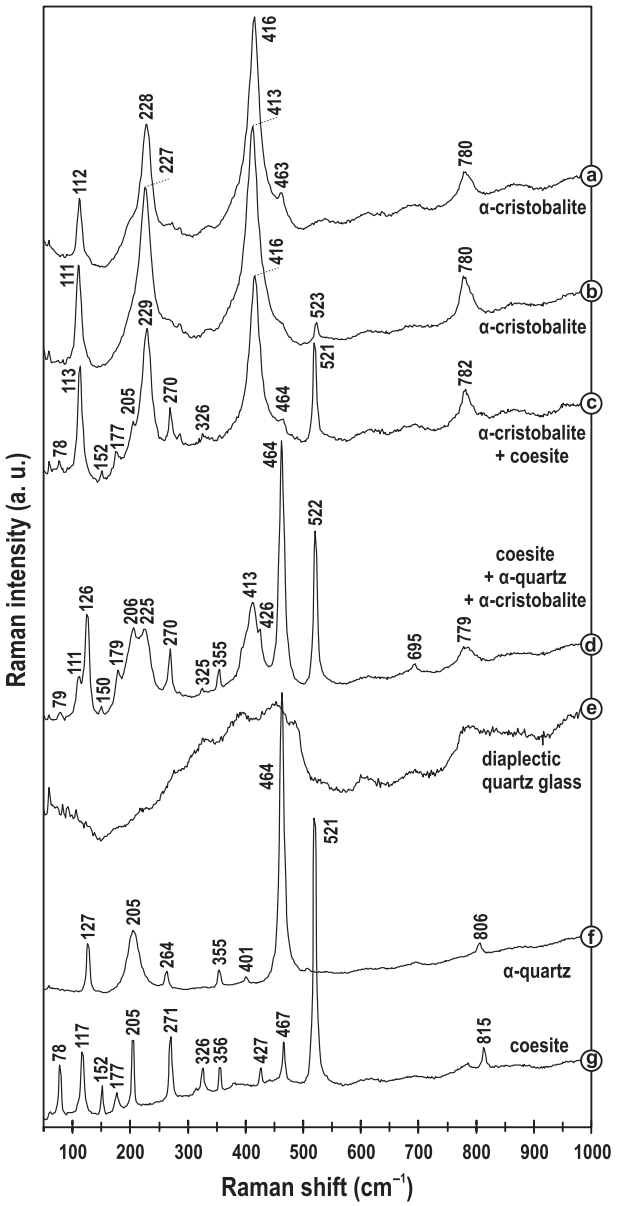

Fig. 7. Selected micro-Raman spectra of different silica phases characteristic of, or associated with, ballen silica. The numbers denote peak positions in cm^{-1}. (a) Alpha-cristobalite spectrum of individual ballen from Mien (sample Mien_02b). (b) Typical α-cristobalite spectrum of individual ballen from Bosumtwi (sample LB-44B2). (c–d) Spectra of minute intra-ballen inclusions, (c) α-cristobalite + coesite spectrum (sample LB-44B) and (d) coesite + α-quartz + α-cristobalite spectrum (sample LB-44B2). (e) Diaplectic quartz glass spectrum. The relatively high background is due to the high degree of amorphisation (sample LB-44B). (f) Typical α-quartz spectrum (sample SIE-9766 from the Ries). Identical α-quartz spectra were obtained for individual ballen from the other impact structures investigated in this study (with the notable exception of the Bosumtwi samples, for which all ballen were found to be composed of α-cristobalite). (g) Spectrum of an aggregate of coesite illustrated in Fig. 5a (sample LB-44B).

impact structures (Fig. 7a, b, respectively) and show the four peaks typical for α-cristobalite at 111–113, 227–229, 413–416, and 780–782 cm^{-1} (*e.g.*, Bates, 1972). All the ballen in Bosumtwi samples consist of α-cristobalite. However, in the case of the Mien samples, only a few α-cristobalite ballen have been observed together with ballen made of α-quartz, occurring in the same silica inclusion. Ballen from the other investigated impact structures are only composed of α-quartz and have a typical α-quartz Raman signature easily identified based on its intense Raman line at 464 cm^{-1} (Fig. 7f).

Raman spectra of different portions of the same ballen were acquired and show no significant differences, indicating the absence of intraballen variations (in agreement with the SEM results). Some α-cristobalite ballen (type I) contain coesite in the form of tiny, highly refractive, and light green intraballen inclusions (Fig. 5c). These inclusions display the characteristic Raman peaks of coesite, but the bands of α-cristobalite and/or α-quartz occur in these spectra as well (Fig. 7b, c). The mixture of coesite ± α-cristobalite results from the minimum size of the Raman light beam, which is somewhat larger than the analyzed coesite crystals. The occurrence of α-quartz together with coesite within cristobalite ballen can be explained by the presence of some remnant quartz crystals due to initial shock heterogeneity on the sub-crystal scale, or alternatively by partial back-transformation of coesite to α-quartz. For comparison, Raman spectra of a coesite aggregate and of the host diaplectic quartz glass are also shown (Fig. 7g, e, respectively).

4.4. Transmission electron microscopy

The TEM observations on a FIB foil, cut across the triple junction between three α-cristobalite ballen, revealed that ballen are formed of numerous highly twinned crystals with different crystallographic orientations (Fig. 8). Crystals display polysynthetic twinning with extremely thin twin lamellae and sharp angular contacts between them (Fig. 9). Individual crystals of α-cristobalite are up to 2 μm long. The observed complex twinning and very small size of the crystals are typical for α-cristobalite that has been back-transformed from high temperature β-cristobalite (*e.g.*, Deer *et al.*, 2004). The contact zones of the investigated α-cristobalite ballen are marked by the occurrence of fibrous material (*i.e.*, phyllosilicates), which probably precipitated in interstices between individual silica ballen or resulted from the aqueous alteration of glass phases. Energy-dispersive X-ray microanalysis showed that these phyllosilicates are Al- and Fe-rich (Al/Si ratio ~0.4–0.5; Al/Fe ratio ~2.2–2.3) and contain a minor amount of Ca (Fig. 9). Based on X-ray diffraction analysis, this badly crystallized phyllosilicate material, with basal d-spacing increasing from 14 to 16.5 Å after saturation with ethylene glycol, probably belongs to the smectite group (Fe-smectite?) (S. Gier, Unir. Vienna, pers. comm.).

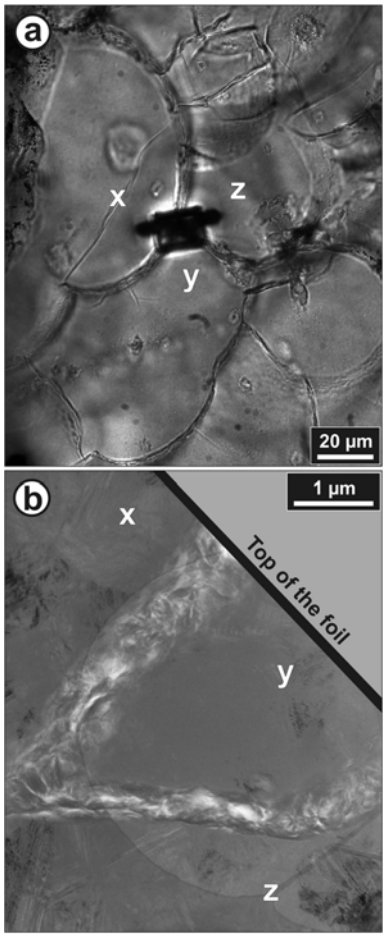

Fig. 8. (a) Microphotograph (in plane-polarized light) with the exact location of the FIB preparation of the TEM foil. The three ballen in contact are noted ''x'', ''y'', and ''z'' for orientation. (b) Overview TEM bright field image of the upper part of the TEM foil. Fibrous material (phyllosilicate mineral) occurs between ballen made of pure SiO_2. The light grey network shown in the background corresponds to the carbon grid supporting the specimen. Sample LB-44B from the Bosumtwi crater.

5. Discussion and summary

5.1. Ballen characteristics and occurrences

Ballen are not cracks or vacuoles, but more or less spheroidal bodies, like grapes, which interpenetrate each other or abut each other. Ballen appear to be spheroids and not lamellae (previously proposed by Holst, 1890; Short, 1970), because under the microscope, no ''flat'' ballen were observed after investigation of clasts from which thin sections with different orientations had been prepared. ''Ballen texture'' has been described in the literature as a fish-scale pattern (*e.g.*, Whitehead *et al.*, 2002; Osinski, 2004; Schmieder & Buchner, 2007), but this comparison is not appropriate, because fish-scales are layered lamellae, whereas ballen are spheroids, and they also do not overlap each other.

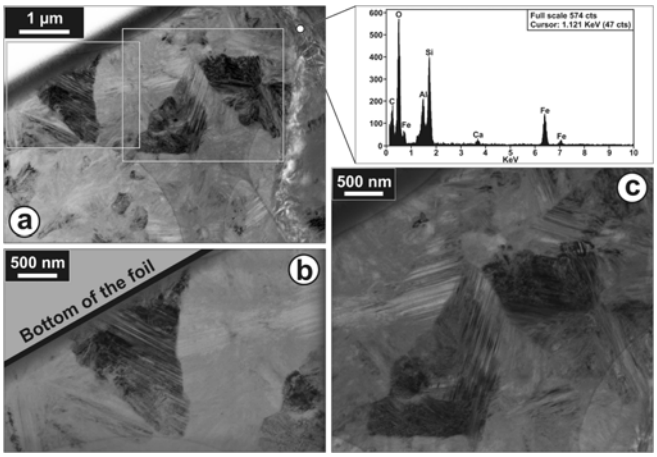

Fig. 9. TEM bright field photomicrographs of α-cristobalite ballen from Bosumtwi (sample LB-44B). (a) General view of a portion of a ballen composed of poly-twinned crystals of α-cristobalite with different orientations. The light grey network shown in this image corresponds to the carbon grid supporting the specimen. The fibrous material filling space between ballen is visible at the right part of the image. The corresponding energy dispersive X-ray spectrum is included. (b–c) Enlarged parts of the general view (a) showing the typical microtexture and arrangement of α-cristobalite crystals forming individual ballen. Note the prominent twin lamellae of the crystals and the sharp angular contact between the crystals.

Individual ballen show a sharp rim, clearly visible with the optical microscope or the SEM. Average ballen are typically about 50 µm wide, but the overall size variation, from 8 to 214 µm, is much larger. The size distribution from inclusion to inclusion (*i.e.*, diaplectic quartz glass or lechatelierite inclusion) is also highly variable, ranging from inclusions with ballen of homogeneous size to inclusions with a large ballen size variation. Large ballen may in some inclusions occur preferentially in the peripheral area, but they may also be present in the central part of a silica inclusion.

Optical observations and Raman spectroscopy have revealed the occurrence of tiny, often light green to brownish inclusions of coesite within ballen of type I (Fig. 2e and 5c; Table 2). Concerning ballen of types II, III, IV, and V (Table 2), no coesite inclusions have been observed so far, but tiny internal defects occur within ballen α-quartz.

Ballen are composed of two polymorphs of silica, α-cristobalite and α-quartz, and more rarely coesite occurs in the form of tiny intraballen inclusions in α-cristobalite ballen (so far only observed/preserved in ballen from the Bosumtwi; Fig. 2e and 5c). Tridymite was also identified by X-ray diffraction in ballen-quartz-bearing melt rocks from the Popigai structure (Vishnevsky & Montanari, 1999; Whitehead *et al.*, 2002), but not in any of our samples. Moreover, considering that tridymite was not observed in situ in ballen and without proper details regarding its relation to other polymorphs of silica, it is difficult to interpret the occurrence of tridymite in ballen silica.

The TEM investigations confirmed the presence of phyllosilicates between individual ballen. We interpret these phyllosilicates as evidence of fluid circulation; possibly, these phyllosilicate minerals filled void spaces between individual ballen.

The presence of relics of PDFs within ''ballen quartz'', described from experimentally produced ballen (*e.g.*, Rehfeldt-Oskierski, 1986), has not been found in any of our samples. However, quartz glass clasts with both ballen silica and crystalline relic areas with PDFs have been observed (*e.g.*, at the Mien impact structure). Ballen with a ''toasted appearance'', somewhat similar to what has been described for shocked quartz grains (*e.g.*, Short & Gold, 1996), have been noted in impact melt samples from the Popigai (Whitehead *et al.*, 2002) and Dhala (Pati *et al.*, in press) impact structures but not in our samples.

Ballen silica occurs in impact melt rock, as well as in suevite, and in both cases, ballen are irregularly distributed at the sample scale.

5.2. Ballen formation and phase transformation processes

Shock transformation and deformation of quartz have been studied extensively (*e.g.*, Stöffler & Langenhorst, 1994; Grieve *et al.*, 1996; and references therein). It is well known that diaplectic glass starts to form in the solid state in the form of distinct lamellae (*i.e.*, PDFs) along crystallographic orientations (from ~10 GPa; *e.g.*, Stöffler & Langenhorst, 1994). At higher pressures (~35 GPa), quartz is totally amorphized and forms so-called diaplectic quartz glass (Fig. 6). Quartz melts at higher pressure (~50 GPa). However, lechatelierite (the mono-mineralic quartz melt) can form at very high temperatures (above 1700 °C), without necessarily requiring high shock pressures (Fig. 6). Lechatelierite occurs in nature only in fulgurites (*e.g.*, Rogers, 1928, 1946) and in impactites (*e.g.*, Stöffler & Langenhorst, 1994; and references therein).

During our investigations, ballen have been observed in both diaplectic quartz glass and lechatelierite inclusions. This means that two processes of formation of ballen are operative: (1) a solid-solid transition, from α-quartz to diaplectic quartz glass and then formation/crystallisation at high temperature of ballen of β-cristobalite and/or β-quartz states, and finally back-transformation to α-cristobalite and/or α-quartz, and (2) a solid-liquid transition, from α-quartz to lechatelierite and then nucleation and growth of β-cristobalite and/or β-quartz ballen at high temperatures that are then back-transformed to α-cristobalite and/or α-quartz.

Ballen at the embryonic stage have been observed at the edges of grains and along fractures (Fig. 2 and 5a), but also around inclusions and other defects preserved in the glass (Fig. 5b). These observations are in good agreement with the fact that defects or impurities are essential for inducing the nucleation of β-cristobalite (*e.g.*, Shoval *et al.*, 1997).

The tiny inclusions of coesite observed within α-cristobalite ballen (Fig. 2e and 5c) also represent possible nuclei for the nucleation of β-cristobalite ballen.

Pure silica is readily transformed into β-cristobalite at temperatures between 1470 and 1710 °C (Fig. 6); however, in natural silica minerals this transformation has been observed at comparatively lower temperatures between 1100–1600 °C (*e.g.*, Shoval *et al.*, 1997). This may be due to the presence of trace elements. In addition, water content and pressure conditions affect the temperature range. In high-temperature annealing experiments with diaplectic quartz glass, ''ballen like'' features started to form at about 1200 °C (Short, 1970; Rehfeldt-Oskierski, 1986).

Concerning the ballen types II, III, IV, and V (see Table 2), all composed of α-quartz, it is probable that these ballen, originally formed as β-cristobalite or β-quartz, were then back-transformed to α-quartz with time. Beta-cristobalite, which is only metastable at ambient temperature, slowly converts to the quartz structure with time (*e.g.*, Heaney, 1994). The occurrence of α-cristobalite ballen (type I), together with ballen α-quartz in the same silica inclusions from the Mien impact structure, is considered as evidence that the transformation from α-cristobalite to α-quartz has taken place. In addition, the observation that only α-cristobalite ballen occur at the relatively young (1.07 Ma old) Bosumtwi crater seems to support this interpretation. In terms of volume change, the transformation of cristobalite phases to α-quartz corresponds to a volume shrinkage of about 12 % (at atmospheric pressure; *e.g.*, Hemley *et al.*, 1994; and references therein). The transformation of cristobalite phases to α-quartz and the conditions (*e.g.*, velocity, water content, stress, etc) of this transformation evidently influence the formation of the different types (II, III, IV, and V) of ballen silica. However, we assume that these differences are mostly a function of the respective *P–T* conditions and velocity of the transformation of cristobalite phases to α-quartz. The volume changes resulting from the transformation of cristobalite polymorphs to α-quartz can also influence the orientations of nuclei (Wheeler *et al.*, 2001), inducing some misorientations of the resulting α-quartz crystals within ballen. In addition, post-impact alteration processes have also affected ballen silica, illustrated by the presence of phyllosilicate minerals in between ballen.

Nevertheless, it is not clear whether post-impact alteration processes (*e.g.*, hydrothermal alteration) directly influence microstructures of the different ''ballen quartz'' types. The exact conditions of formation for the different types of ballen (types II, III, IV, and V) are still unclear. Some annealing experiments and detailed petrographic observations of the resulting ballen-like features are necessary to better understand the transformation of cristobalite polymorphs to α-quartz and the various textures and microstructures observed in natural ballen. In addition, the observed size ranges and heterogeneous size distributions of ballen within silica inclusions, as well as the variety of ballen shapes, must have implications regarding ballen formation. As discussed previously, impurities are necessary for the nucleation of β-cristobalite (*e.g.*, Shoval *et al.*, 1997), and consequently the distribution of ballen within silica clasts is mostly influenced by the distribution of initial impurities or other lattice defects, as nucleation sites. On the other hand, temperature gradients across clasts and cooling rates will influence the size ranges of ballen within silica inclusions. The different shapes of ballen observed during our study can either be the result of growing under stress conditions, or a function of the characteristics of the nuclei.

The occurrence of ballen quartz/cristobalite in suevite samples, such as at the Bosumtwi and at the Chicxulub impact structures, has interesting implications in terms of timing of formation and for the quantification of the cooling history of suevite deposits. We have shown that the different types of ballen are mostly a function of the *P–T* conditions, and that is why the occurrence of the different types of ballen (as at the Bosumtwi; exclusively of type I) in suevite samples can possibly be used as a tracer of these conditions (*i.e.*, remnant temperature of suevite deposits). The maximum size of ballen can also give some information on the duration of the conditions permitting the growth of ballen. However, as already discussed for the effects of post-impact alteration processes on the different types of ballen, further annealing experiments are necessary.

5.3. Ballen quartz/cristobalite – evidence for shock metamorphism?

Quartz is one of the most commonly used indicator minerals for shock metamorphism, as well as for pressure calibration. Quartz displays a wide variety of shock-induced mechanical deformations and transformations: PFs, PDFs, mosaicism, transformation to coesite and stishovite, amorphisation (*i.e.*, formation of diaplectic glass), and melting (*e.g.*, Stöffler, 1971; Stöffler & Langenhorst, 1994; Grieve *et al.*, 1996; Huffman & Reimold, 1996; Stähle *et al.*, 2008; and references therein).

Our observations have shown that ballen quartz/cristobalite is formed from diaplectic quartz glass and lechatelierite, nucleating at high temperatures (Fig. 6). Obviously, the formation of ballen silica requires special conditions, because otherwise such features would be abundant in volcanic rocks.

Recently, in an abstract, Schmieder & Buchner (2007) suggested that ''ballen quartz'' might not be restricted to impactites, claiming that similar features could occur in volcanic rocks and in fulgurites. It is well known (*e.g.*, Rogers, 1928; Deer *et al.*, 2004) that β-cristobalite, a high-temperature polymorph of silica, is common in acidic volcanic rocks, usually in the form of minute octahedrons, radiating clusters, spherical aggregates, or spherulites intergrown with feldspar. Schmieder & Buchner (2007) referred to a paper by Swanson *et al.* (1989) that mentions the occurrence of poikilitic cristobalite filling the space between feldspar fibres in obsidian. Ballen-like features were, however, not mentioned by Swanson *et al.* (1989).

Cristobalite in this case appears to have nucleated after feldspar, individual crystals of cristobalite are very small (<10 μm), and the presence of coesite was not reported. The particular petrographic contexts of occurrence of these cristobalite ''crystals'', as well as their characteristics, are very different from α-cristobalite ballen (type I) described in our study. In addition, in the case of silica glass (*i.e.*, obsidian) inclusions that occur in volcanic rocks, obsidian is not composed of pure SiO_2, but contains a certain amount of other oxides such as Al_2O_3, K_2O, or NaO. Ballen quartz/cristobalite has so far only been observed within pure SiO_2 inclusions (*i.e.*, diaplectic quartz glass and lechatelierite) in impactites.

Concerning the alleged occurrence of ballen-like features in fulgurites formed in quartz-rich sand, Schmieder & Buchner (2007) referred to a paper by Rogers (1946), where the occurrence of cristobalite is mentioned, but the presence of ballen-like features was actually not described. Mostly made of silica glass (*i.e.*, lechatelierite), sand fulgurites show remnants of quartz grains and abundant vesicles (generally empty) within a glassy matrix. Rarely cristobalite occurs in the external part of the fulgurite (*e.g.*, Rogers, 1946), but, so far, no α-cristobalite or α-quartz ballen have been described from fulgurites. Considering also the extremely short duration of the high-temperatures (above 1700 °C; Essene & Fisher, 1986) involved in the formation of sand fulgurites, it is not conceivable that cristobalite crystals can develop more than a few micrometers in size. The slower cooling rate within high-temperature impactites might be a requirement to form ballen. As in the case of cristobalite in volcanic rocks, the context of occurrence of cristobalite in sand fulgurites is, in any case, not comparable to α-cristobalite ballen in impactites.

We have shown that ballen silica occurs exclusively within diaplectic quartz glass and lechatelierite inclusions (*i.e.*, pure silica glass), phases that form at high shock pressures, namely ~35 and ~50 GPa, respectively (Fig. 6; *e.g.*, Stöffler & Langenhorst, 1994). Moreover, the temperature must have exceeded ~1200–1400 °C, according to annealing experiments by Short (1970) and Rehfeldt-Oskierski (1986). Only shock metamorphism can reach these *P–T* conditions at the Earth's surface. However, as ballen quartz/cristobalite are the result of back-transformations from shock-induced states, ballen silica cannot be considered direct evidence of shock metamorphism; however, its occurrence is restricted to impact-derived rocks and, thus, its presence should be added to the list of impact-characteristic criteria.

6. Conclusions

Investigation of α-quartz and α-cristobalite ballen in 27 thin sections from five different impact structures (Bosumtwi, Chicxulub, Mien, Ries, and Rochechouart), combined with literature data, has shown that ballen occur within diaplectic quartz glass and lechatelierite inclusions, not only in impact melt rock but also in suevite. Our observations show that two processes of formation are operating: (1) a solid-solid transition, from α-quartz to diaplectic quartz glass and then formation of ballen loops made of β-cristobalite and/or β-quartz, and (2) formation by nucleation and crystal growth at high temperatures after lechatelierite formation. In addition, our investigations have indicated that ballen, originally made of β-cristobalite and/or β-quartz, are back-transformed to α-cristobalite and to α-quartz with time. Coesite inclusions were also, for the first time, observed and characterized within ballen silica.

Five types of ballen have been distinguished: α-cristobalite ballen with homogeneous extinction (type I); ballen α-quartz with homogeneous extinction (type II), with heterogeneous extinction (type III), and with intra-ballen recrystallisation (type IV); chert-like recristallized ballen α-quartz (type V).

Since more than 20 years, ''ballen quartz'' has on occasion been used as a ''shock pressure indicator'' (*e.g.*, Dressler *et al.*, 1997; Whitehead *et al.*, 2002), based on the occurrence of the three different types of ballen as described by Bischoff & Stöffler (1984). Our observations indicate that the interpretation of shock pressures cannot be based only on the occurrence of different types of ballen silica, because the different types of ballen are the result from post-impact transformations.

Nevertheless, the presence of ballen quartz/cristobalite provides some constraint on shock pressure which must have exceeded ~35 GPa (pressure of formation of diaplectic quartz glass; *e.g.*, Stöffler & Langenhorst, 1994; and references therein), as well as on temperature at ballen formation, which must have exceeded 1200 °C (based on annealing experiments by Short, 1970 and Rehfeldt-Oskierski, 1986).

Acknowledgements: This work was supported by the Austrian Science Foundation (FWF), grant P18862-N10, and the Austrian Academy of Sciences. We are grateful to F. Brandstätter (Natural History Museum, Vienna, Austria) for assistance with SEM and CL work, to E. Libowitzky (University of Vienna, Austria) for assistance with the micro Raman spectroscopic analyses, S. Gier (University of Vienna, Austria) for an XRD analysis, to S. Augustin and R. Wirth (GFZ, Potsdam, Germany) for the FIB preparation, and to A. Greshake (Museum of Natural History, Humboldt-University, Berlin, Germany) for assistance with the TEM. Thanks also to J-P. Lorand and G. Carlier (Muséum National d'Histoire Naturelle, Paris, France) and to R.-T. Schmitt (Museum of Natural History, Humboldt-University, Berlin, Germany) for providing thin sections from the Rochechouart and Ries craters, respectively, H. Reyss (SAF, Paris, France) and E. Dransart (EMTT, Francheville, France) for the samples from Mien crater, C. Alwmark (University of Lund, Sweden) for providing and translating the reference by Holst (1890), and B. and M.H.

French, E.P. Gurov, J. Morrow, D. Stöffler, and A. Wittmann for helpful and constructive discussions. We thank J. Spray and two anonymous reviewers for constructive comments on an earlier version of this manuscript.

References

Åström, K. (1998): Seismic signature of the Lake Mien impact structure, southern Sweden. *Geophys. J. Int.*, **135**, 215–231.

Bartosova, K., Ferrière, L., Koeberl, C., Reimold, W.U., Gibson, R., Schmitt, R.T. (2007): Lithological, petrographical, and geochemical investigations of suevite from the Eyreville core, Chesapeake Bay impact structure. *Geol. Soc. Am. Abst. Prog.*, **39**, A451.

Bates, J.B. (1972): Raman spectra of α and β cristobalite. *J. Chem. Phys.*, **57**, 4042–4047.

Bischoff, A. & Stöffler, D. (1984): Chemical and structural changes induced by thermal annealing of shocked feldspar inclusions in impact melt rocks from Lappajärvi crater, Finland. *J. Geophys. Res.*, **89**, B645–B656.

Boamah, D. & Koeberl, C. (2006): Petrographic studies of fallout suevite from outside the Bosumtwi impact structure, Ghana. *Meteorit. Planet. Sci.*, **41**, 1761–1774.

Boyer, H., Smith, D.C., Chopin, C., Lasnier, B. (1985): Raman microprobe (RMP) determinations of natural and synthetic coesite. *Phys. Chem. Minerals*, **12**, 45–48.

Buchner, E., Seyfried, H., van den Bogaard, P. (2003): $^{40}Ar/^{39}Ar$ laser probe age determination confirms the Ries impact crater as the source of glass particles in Graupensand sediments (Grimmelfingen Formation, North Alpine Foreland Basin). *Int. J. Earth Sci.*, **92**, 1–6.

Carstens, H. (1975): Thermal history of impact melt rocks in the Fennoscandian shield. *Contrib. Mineral. Petrol.*, **50**, 145–155.

Cohen, L.H. & Klement, W.K., Jr. (1967): High-low quartz inversion: determination to 35 kilobars. *J. Geophys. Res.*, **73**, 4245–4251.

Coney, L., Gibson, R.L., Reimold, W.U., Koeberl, C. (2007): Lithostratigraphic and petrographic analysis of ICDP drill core LB-07A, Bosumtwi impact structure, Ghana. *Meteorit. Planet. Sci.*, **42**, 569–589.

Deer, W.A., Howie, R.A., Wise, W.S., Zussman, J. (2004): Rock-forming minerals. Framework silicates: silica minerals, feldspathoids and the zeolites, The Geological Society, London, Vol. 4B, 2nd edition, 982 p.

Dressler, B.O., Crabtree, D., Schuraytz, B.C. (1997): Incipient melt formation and devitrification at the Wanapitei impact structure, Ontario, Canada. *Meteorit. Planet. Sci.*, **32**, 249–258.

Earth Impact Database. (2008): http://www.unb.ca/passc/ImpactDatabase/ (accessed 15 December 2007).

Engelhardt, W. von (1972): Shock produced rock glasses from the Ries crater. *Contrib. Mineral. Petrol.*, **36**, 265–292.

Engelhardt, W. von & Stöffler, D. (1968): Stages of shock metamorphism in the crystalline rocks of the Ries Basin (Germany). *in* ''Shock metamorphism of natural materials'', B.M. French, N.M. Short, eds., Mono Book Corp., Baltimore, 159–168.

Essene, E.J. & Fisher, D.C. (1986) Lightning strike fusion: extreme reduction and metal-silicate liquid immiscibility. *Science*, **234**, 189–193.

Ferrière, L. & Koeberl, C. (2007): Ballen quartz, an impact signature: new occurrence in impact melt breccia at Rochechouart-Chassenon impact structure, France. *Meteorit. Planet. Sci.*, **42**, Suppl, A46.

Ferrière, L., Koeberl, C., Reimold, W.U. (2006): Ballen quartz in impact glass from the Bosumtwi impact crater, Ghana. *Meteorit. Planet. Sci.*, **41**, Suppl, A54.

Ferrière, L., Koeberl, C., Reimold, W.U. (2007): Drill core LB-08A, Bosumtwi impact structure, Ghana: petrographic and shock metamorphic studies of material from the central uplift. *Meteorit. Planet. Sci.*, **42**, 611–633.

French, B.M. (1998): *Traces of catastrophe: a handbook of shock-metamorphic effects in terrestrial meteorite impact structures*. LPI Contrib. No 954, Lunar and Planetary Institute, Houston, 120 p.

French, B.M., Hartung, J.B., Short, N.M., Dietz, R.S. (1970): Tenoumer crater, Mauritania: age and petrologic evidence for origin by meteorite impact. *J. Geophys. Res.*, **75**, 4396–4406.

Grieve, R.A.F. (1975): Petrology and chemistry of the impact melt at Mistastin Lake crater, Labrador. *Geol. Soc. Am. Bull.*, **86**, 1617–1629.

Grieve, R.A.F. & Ber, T.J. (1994): Shocked lithologies at the Wanapitei impact structure, Ontario, Canada. *Meteorit. Planet. Sci.*, **29**, 621–631.

Grieve, R.A.F., Reny, G., Gurov, E.P., Ryabenko, V.A. (1987): The melt rocks of the Boltysh impact crater, Ukraine, USSR. *Contrib. Mineral. Petrol.*, **96**, 56–62.

Grieve, R.A.F., Langenhorst, F., Stöffler, D. (1996): Shock metamorphism of quartz in nature and experiment: II. Significance in geoscience. *Meteorit. Planet. Sci.*, **31**, 6–35.

Gurov, E.P., Koeberl, C., Reimold, W.U. (1998): Petrography and geochemistry of target rocks and impactites from the Ilyinets Crater, Ukraine. *Meteorit. Planet. Sci.*, **33**, 1317–1333.

Gurov, E.P., Gurova, E.P., Sokur, T.M. (2002): Geology and petrography of the Zapadnaya impact crater in the Ukrainian shield. *in* ''Impacts in Precambrian shields'', J. Plado, L.J. Pesonen, eds. Impact studies 2, Springer-Verlag, Heidelberg, 173–188.

Gurov, E.P., Koeberl, C., Reimold, W.U., Brandstätter, F., Amare, K. (2005): Shock metamorphism of siliceous volcanic rocks of the El'gygytgyn impact crater (Chukotka, Russia). *in* ''Large meteorite impacts III'', T. Kenkmann, F. Hörz, A. Deutsch, eds. *Geol. Soc. Am. Spec. Paper*, **384**, 391–412.

Heaney, P.J. (1994): Structure and chemistry of the low-pressure silica polymorphs. *in* ''Silica: physical behavior, geochemistry and materials applications'', P.J. Heaney, C.T. Prewitt, G.V. Gibbs, eds. Mineral. Soc. Am., Washington DC. *Rev. Mineral.*, **29**, 1–40.

Hemley, R.J., Prewitt, C.T., Kingma, K.J. (1994): High-pressure behavior of silica. *in* ''Silica: physical behavior, geochemistry and materials applications'', P.J. Heaney, C.T. Prewitt, G.V. Gibbs, eds. Mineral. Soc. Am., Washington DC. *Rev. Mineral.*, **29**, 41–81.

Hildebrand, A.R., Penfield, G.T., Kring, D.A., Pilkington, M., Camargo Zanoguera, A., Jacobsen, S.B. (1991): Chicxulub crater: a possible Cretaceous/Tertiary boundary impact crater on the Yucatán Peninsula, Mexico. *Geology*, **19**, 867–871.

Holst, N.O. (1890): Ryoliten vid sjön Mien. Sveriges Geologiska Undersökning. Serie C, Avhandlingar och uppsatser, No 110. Stockholm, 50 p. (in Swedish).

Huffman, A.R. & Reimold, W.U. (1996): Experimental constraints on shock-induced microstructures in naturally deformed silicates. *Tectonophys.*, **256**, 165–217.

Jackson, I. (1976): Melting of silica isotypes SiO_2, BeF_2 and GeO_2 at elevated pressures. *Phys. Earth Planet. Int.*, **13**, 218–231.

Kanzaki, M. (1990): Melting of silica up to 7 GPa. *J. Am. Ceram. Soc.*, **73**, 3706–3707.

Karikari, F., Ferrière, L., Koeberl, C., Reimold, W.U., Mader, D. (2007): Petrography, geochemistry, and alteration of country rocks from the Bosumtwi impact structure, Ghana. *Meteorit. Planet. Sci.*, **42**, 513–540.

Kelley, S.P. & Spray, J.G. (1997): A late Triassic age for the Rochechouart impact structure, France. *Meteorit. Planet. Sci.*, **32**, 629–636.

Koeberl, C. & Reimold, W.U. (2005): Bosumtwi impact crater, Ghana (West Africa): an updated and revised geological map, with explanations. *Jb. Geol. Bundesanstalt, Wien*, **145**, 31–70.

Kraut, F. (1970): Über ein neues Impaktit-vorkommen im Gebiete von Rochechouart-Chassenon (Départements Haute Vienne und Charente, Frankreich). *Geol. Bavarica*, **61**, 428–450.

Kraut, F. & French, B.M. (1971): The Rochechouart meteorite impact structure, France: preliminary geological results. *J. Geophys. Res.*, **76**, 5407–5413.

Lambert, P. (1977): Les effets des ondes de choc naturelles et artificielles, et le cratère d'impact de Rochechouart (Limousin – France). Unpublished Habilitation Thesis, University of Paris Sud, Centre d'Orsay, France, 176 p. (in French).

Marvin, U.B. & Kring, D.A. (1992): Authentication controversies and impactite petrography of the New Quebec crater. *Meteorit. Planet. Sci.*, **27**, 585–595.

McIntyre, D.B. (1968): Impact metamorphism at Clearwater lake, Quebec. *in* ''Shock metamorphism of natural materials'', B.M. French, N.M. Short, eds. Mono Book Corp., Baltimore, 363–366.

Montanari, A. & Koeberl, C. (2000): Impact stratigraphy: the Italian record. Lectures notes in earth sciences 93, Springer Verlag, Heidelberg, 364 p.

Müller, N., Hartung, J.B., Jessberger, E.K., Reimold, W.U. (1990): 40Ar-39Ar ages of Dellen, Jänisjärvi, and Sääksjärvi impact craters. *Meteorit. Planet. Sci.*, **25**, 1–10.

Osinski, G.R. (2004): Impact melt rocks from the Ries structure, Germany: an origin as impact melt flows? *Earth Planet. Sci. Lett.*, **226**, 529–543.

Pati, J.K., Reimold, W.U., Koeberl, C., Pati, P. (in press): The Dhala structure, Bundelkhand craton, central India – eroded remnant of a large Paleoproterozoic impact structure. *Meteorit. Planet. Sci.*

Pesonen, L.J., Lehtinen, M., Deutsch, A., Elo, S., Lukkarinen, H. (1996): New geophysical and petrographic results of the Suvasvesi N impact structure, Finland (abstract). *Lunar Planet. Sci. Conf.*, **XXVII**, 1021–1022.

Phinney, W.C., Simonds, C.H., Cochran, A., McGee, P.E. (1978): West clearwater, Quebec impact structure, part II: petrology. *Proc. Lunar Planet. Sci. Conf.*, **IX**, 2659–2693.

Pohl, J., Stöffler, D., Gall, H., Ernstson, K. (1977): The Ries impact crater. *in* ''Impact and explosion cratering'', D.J. Roddy, R.O. Pepin, R.B. Merrill, eds. Pergamon, New York, 343–404.

Rehfeldt-Oskierski, A. (1986): Stosswellenexperimente an Quartzeinkristallen und thermisches Verhalten von diaplektischen Quarzgläsern. Unpublished Ph.D. Thesis, University of Münster, Germany, 145 p. (in German).

Reimold, W.U., Koeberl, C., Brandstätter, F., Kruger, F.J., Armstrong, R.A., Bootsman, C. (1999): Morokweng impact structure, South Africa: geologic, petrographic, and isotopic results, and implications for the size of the structure. *in* ''Large meteorite impacts and planetary evolution II'', B.O. Dressler, V.L. Sharpton, eds., *Geol. Soc. Am. Spec. Paper*, **339**, 61–90.

Rogers, A.G. (1928): Natural history of the silica minerals. *Am. Mineral.*, **13**, 73–92.

— (1946): Sand fulgurites with enclosed lechatelierite from riverside country, California. *J. Geol.*, **54**, 117–122.

Schmieder, M. & Buchner, E. (2007): Is ''ballen quartz'' diagnostic for shock metamorphism? *Geochim. Cosmochim. Acta*, **71**, A897.

Short, N.M. (1970): Progressive shock metamorphism of quartzite ejecta from the Sedan nuclear explosion crater. *J. Geol.*, **78**, 705–723.

Short, N.M. & Gold, D.P. (1996): Petrography of shocked rocks from the central peak at the Manson impact structure. *in* ''The Manson impact structure, Iowa: anatomy of an impact crater'', C. Koeberl, R.R. Anderson, eds. *Geol. Soc. Am. Spec. Paper*, **302**, 245–265.

Shoval, S., Champagnon, B., Panczer, G. (1997): The quartz-cristobalite transformation in heated chert rock composed of micro and crypto-quartz by micro-Raman and FT-IR spectroscopy methods. *J. Therm. Anal.*, **50**, 203–213.

Stähle, V., Altherr, R., Koch, M., Nasdala, L. (2008): Shock-induced growth and metastability of stishovite and coesite in lithic clasts from suevite of the Ries impact crater (Germany). *Contrib. Mineral. Petrol.*, **155**, 457–472.

Stöffler, D. (1971): Coesite and Stishovite in shocked crystalline rocks. *J. Geophys. Res.*, **76**, 5474–5488.

Stöffler, D. & Grieve, R.A.F. (2007): Impactites, Chapter 2.11. *in* ''Metamorphic rocks: a classification and glossary of terms, Recommendations of the International Union of Geological Sciences'', D. Fettes, J. Desmons, eds., Cambridge Univ. Press, Cambridge, 82–92, Glossary.

Stöffler, D. & Langenhorst, F. (1994): Shock metamorphism of quartz in nature and experiment: I. Basic observation and theory. *Meteorit. Planet. Sci.*, **29**, 155–181.

Stöffler, D., Artemieva, N.A., Ivanov, B.A., Hecht, L., Kenkmann, T., Schmitt, R.T., Tagle, R.A., Wittmann, A. (2004): Origin and emplacement of the impact formations at Chicxulub, Mexico, as revealed by the ICDP deep drilling at Yaxcopoil-1 and by numerical modeling. *Meteorit. Planet. Sci.*, **39**, 1035–1067.

Swanson, S.E., Naney, M.T., Westrich, H.R., Eichelberger, J.C. (1989): Crystallization of Obsidian Dome, Inyo Domes, California. *Bull. Volcanol.*, **51**, 161–176.

Thomas, M.D., Innes, M.J.S., Dence, M.R., Grieve, R.A.F., Robertson, P.B. (1977): Gow Lake, Saskatchewan: evidence for an origin by meteorite impact. *Meteoritics*, **12**, A370–371.

Tuchscherer, M.G., Reimold, W.U., Koeberl, C., Gibson, R.L., de Bruin, D. (2004): First petrographic results on impactites from the Yaxcopoil-1 borehole, Chicxulub structure, Mexico. *Meteorit. Planet. Sci.*, **39**, 899–930.

Vishnevsky, S. & Montanari, A. (1999): Popigai impact structure (Arctic Siberia, Russia): geology, petrology, geochemistry, and geochronology of glass-bearing impactites. *in* ''Large meteorite impacts and planetary evolution II'', B.O. Dressler, V.L. Sharpton, eds., *Geol. Soc. Am. Spec. Paper*, **339**, 19–59.

Wheeler, J., Prior, D.J., Jiang, Z., Spiess, R., Trimby, P.W. (2001): The petrological significance of misorientations between grains. *Contrib. Mineral. Petrol.*, **141**, 109–124.

Whitehead, J., Grieve, R.A.F., Spray, G. (2002): Mineralogy and petrology of melt rocks from the Popigai impact structure, Siberia. *Meteorit. Planet. Sci.*, **37**, 623–647.

Wirth, R. (2004): Focused Ion Beam (FIB): a novel technology for advanced application of micro- and nanoanalysis in geosciences and applied mineralogy. *Eur. J. Mineral.*, **16**, 863–876.

Wittmann, A., Kenkmann, T., Schmitt, R.T., Hecht, L., Stöffler, D. (2004): Impact-related dike breccia lithologies in the ICDP drill core Yaxcopoil-1, Chicxulub impact structure, Mexico. *Meteorit. Planet. Sci.*, **39**, 931–954.

Zhang, J., Liebermann, R.C., Gasparik, T., Herzberg, C.T., Fei, Y. (1993): Melting and subsolidus relations of SiO_2 at 9–14 GPa. *J. Geophys. Res.*, **98**, 19785–19793.

Received 15 July 2008
Modified version received 30 July 2008
Accepted 1 September 2008